A

```
  1 MAPIKEFISK FSDFKNNKKL ILSSAAIALL LLASIVGIAA TTTNQNKNQK ITTLSSTSHA
                                                FL    Δ4   Δ8
 61 ILKSVCSSTL YPELCFSAVA ATGGKELTSQ KEVIEASLNL TTKAVKHNYF AVKKLIAKRK
    Δ12  Δ16  Δ20                  Δ42
121 GLTPREVTAL HDCLETIDET LDELHVAVED LHQYPKQKSL RKHADDLKTL ISSAITNQGT
                                          Δ115
181 CLDGFSYDDA DRKVRKALLK GQVHVEHMCS NALAMIKNMT ETDIANFELR DKSSTFTNNN
                                                      Δ192
241 NRKLKEVTGD LDSDGWPKWL SVGDRRLLQG STIKADATVA DDGSGDFTTV AAAVAAAPEK
                  Δ212                MAT****** ********** **********
301 SNKRFVIHIK AGVYRENVEV TKKKTNIMFL GDGRGKTIIT GSRNVVDGST TFHSATVAAV
                     ***** ***
361 GERFLARDIT FQNTAGPSKH QAVALRVGSD FSAFYQCDMF AYQDTLYVHS NRQFFVKCHI

421 TGTVDFIFGN AAAVLQDCDI NARRPNSGQK NMVTAQGRSD PNQNTGIVIQ NCRIGGTSDL
                                             ** ********** *** *******
481 LAVKGTFPTY LGRPWKEYSR TVIMQSDISD VIRPEGWHEW SGSFALDTLT YREYLNRGGG
     ****** ******
****
541 AGTANRVKWK GYKVITSDTE AQPFTAGQFI GGGGWLASTG FPFSLSL*
```

B

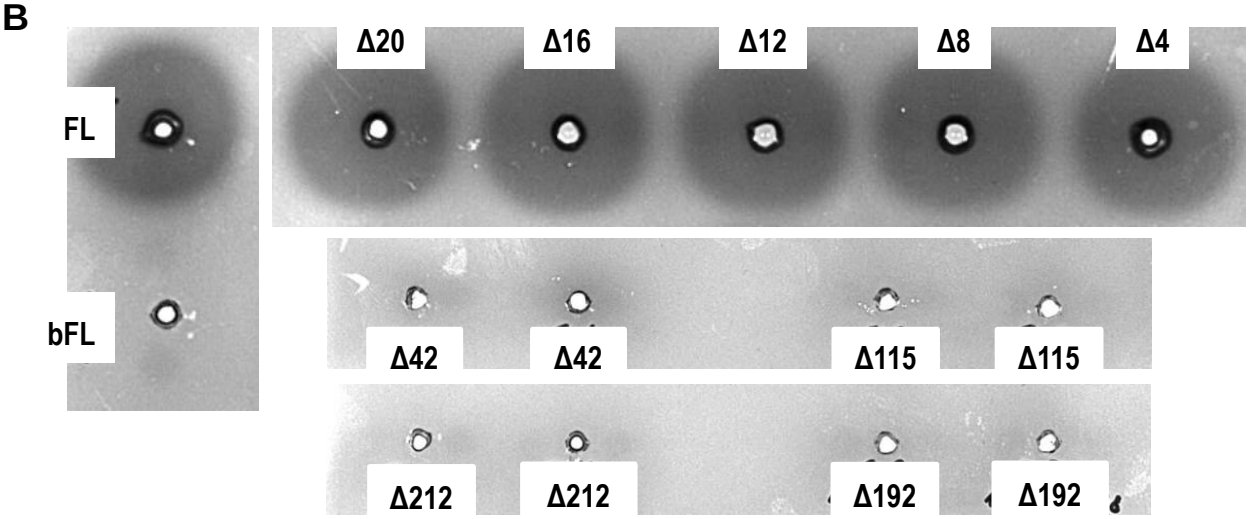

Deletion	FL	Δ4	Δ8	Δ12	Δ16	Δ20	Δ42	Δ115	Δ192	Δ212
Activity	+	+	+	+	+	+	-	-	-	-

Supplemental Figure 1: (A) AtPME2 amino-acid sequence highlighting the sequences used for expression in *Pichia pastoris* (signal peptide in bold, PRO part in green, mature part in cyan and putative processing motifs indicated in red in the intermediate region in yellow, red arrows indicate the different truncated versions). Peptides mapping AtPME2 in cell wall-enriched extracts of Col-0 dark-grown hypocotyls using nano LC-MS/MS are underlined with asterisks. **(B)** Effects of deletion of the N-terminus sequence of AtPME2 on the production of an active enzyme in Pichia. FL: Full length AtPME2, FLb: heat-denaturated AtPME2, Δ4FL to Δ212FL: Deletion of 4 to 212 amino acids of the PRO part. PME activity was assessed on concentrated supernatants using gel diffusion assay.

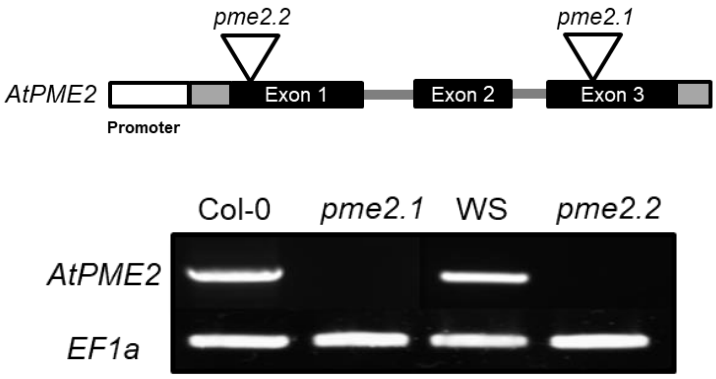

Supplemental Figure 2: Schematic representation of *AtPME2* gene structure and localization of the T-DNA insertions for *pme2-1* (GK-835A09, in the third exon) and *pme2-2* (FLAG_445B05, in the first exon). PCR analysis of *pme2-1*, *pme2-2* and WT (Col-0 and WS) hypocotyl cDNAs using specific primers flanking the T-DNA insertion sites. *EF1α* was used as reference gene.

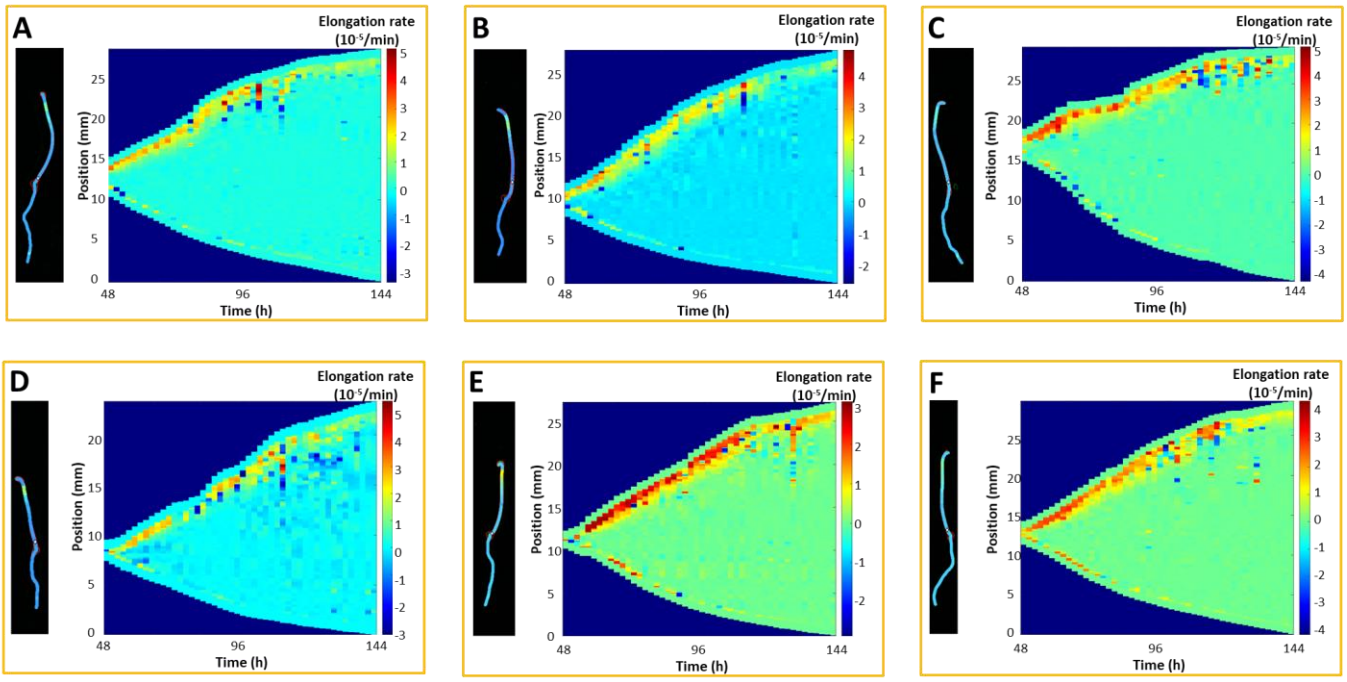

Supplementary figure 3: Elemental relative rates of elongation for 3 wild-type Col-0 **(A-C)** and 3 *pme2-1* seedlings **(D-E)**. In each panel, the colour scale on the left indicates relative increase in length of hypocotyl and root (10^{-5}/min corresponds to 0.001% increase per minute or to 0.06% per hour). Elongation rate is shown along the seedling at 96h on the right. The kymograph in the middle shows elongation rate along the seedling at one time point, with all time points assembled horizontally.

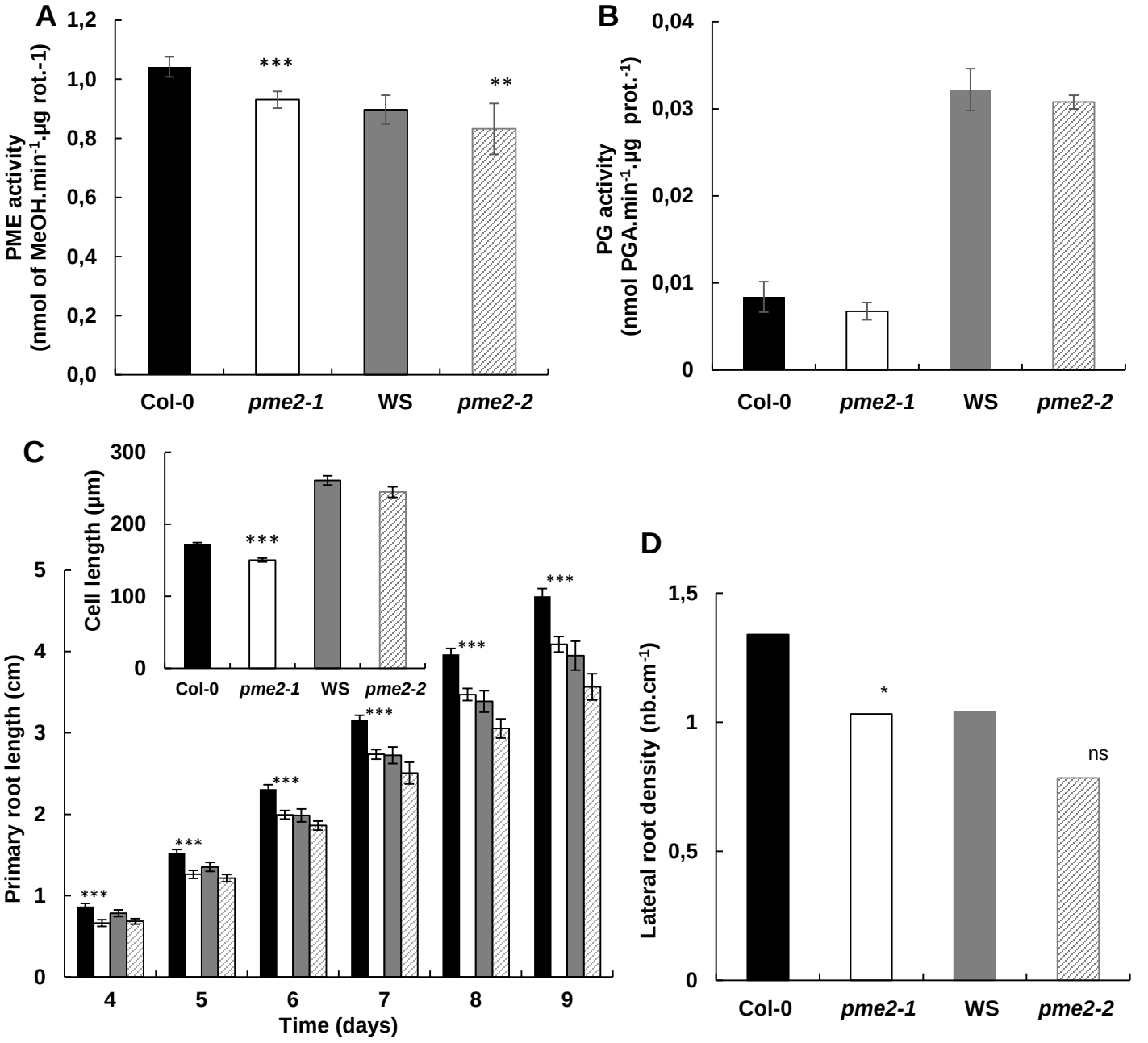

Supplemental Figure 4 : (A) PME activity of cell wall-enriched protein extracts from 7-day-old roots of wild type Col-0/WS and *pme2-1*/*pme2-2* mutants. Data represent the means of PME activity in nmol of methanol.min-1/µg of protein-1± SE of three independent protein extractions and three technical replicates (n=9). **(B)** PG activity of cell wall-enriched protein extracts from 7-day-old roots of wild type Col-0/WS and *pme2-1*/*pme2-2* mutants. Data represent the means of PG activity in nmol of GalA.min-1/µg of protein-1± SE of three independent protein extractions and three technical replicates (n=9). **(A-B)** Significant differences with $p<0.05$ (*), $p < 0.01$ (**), $p < 0.001$ (***), were determined according to Mann-Whitney. **(C)** Time course analysis of root elongation of wild type Col-0 (black bar), WS (grey bar), pme2-1 (white bar) and *pme2-2* (hatched bar). Data represent the means of length, in cm ± SE ($n > 30$), for each condition. Inset: Length of fully elongated cells of 7-day-old roots measured between two root hairs. 300 cells were measured for each condition. Significant differences were determined according to a Student t-test with $p < 0.001$ (***). **(D)** Lateral root density of wild type Col-0 (black bar), WS (grey bar), pme2-1 (white bar) and pme2-2 (hatched bar). Data represent the means ± SE ($n > 30$), for each condition. Significant differences were determined according to a Student t-test with $p<0.05$ (*).

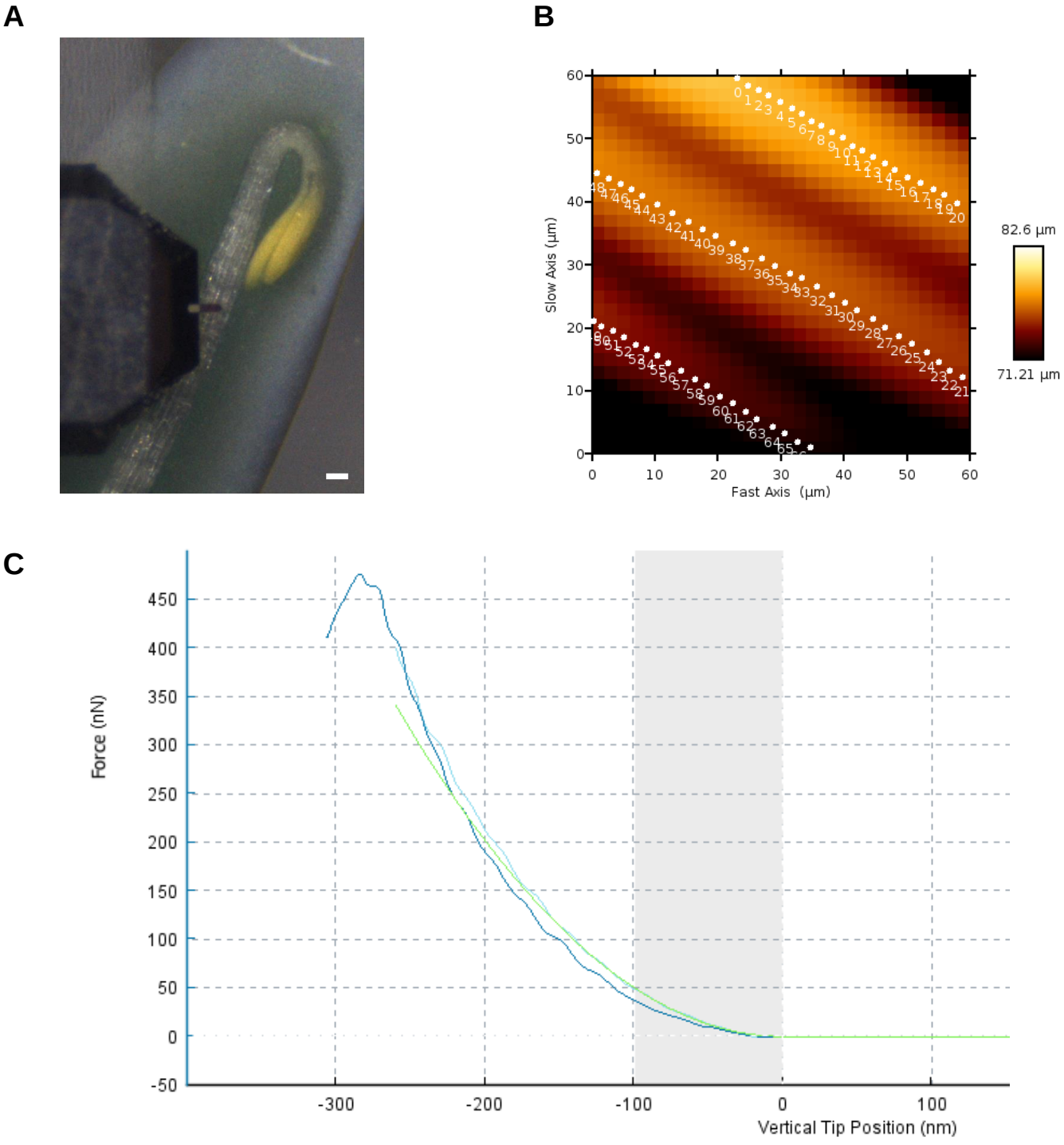

Supplemental Figure 5: AFM analysis of 3-day-old hypocotyls. **(A)** Top view of a wild-type hypocotyl under the atomic force microscope; the cantilever (rectangular with a triangular end) is located over the hypocotyl at about 1mm from the hook. Scale bar 100 µm. **(B)** Topographic image of a 60 µm x 60 µm region of the hypocotyl (height scale on right), with three cells partially visible. The white dots show points where force-depth curves were obtained in order to characterise cell wall stiffness. **(C)** Typical force-depth curve with approach in light blue, retract in dark blue. The green curve is a fit of the approach to the Sneddon model, which yields the apparent Young's modulus.

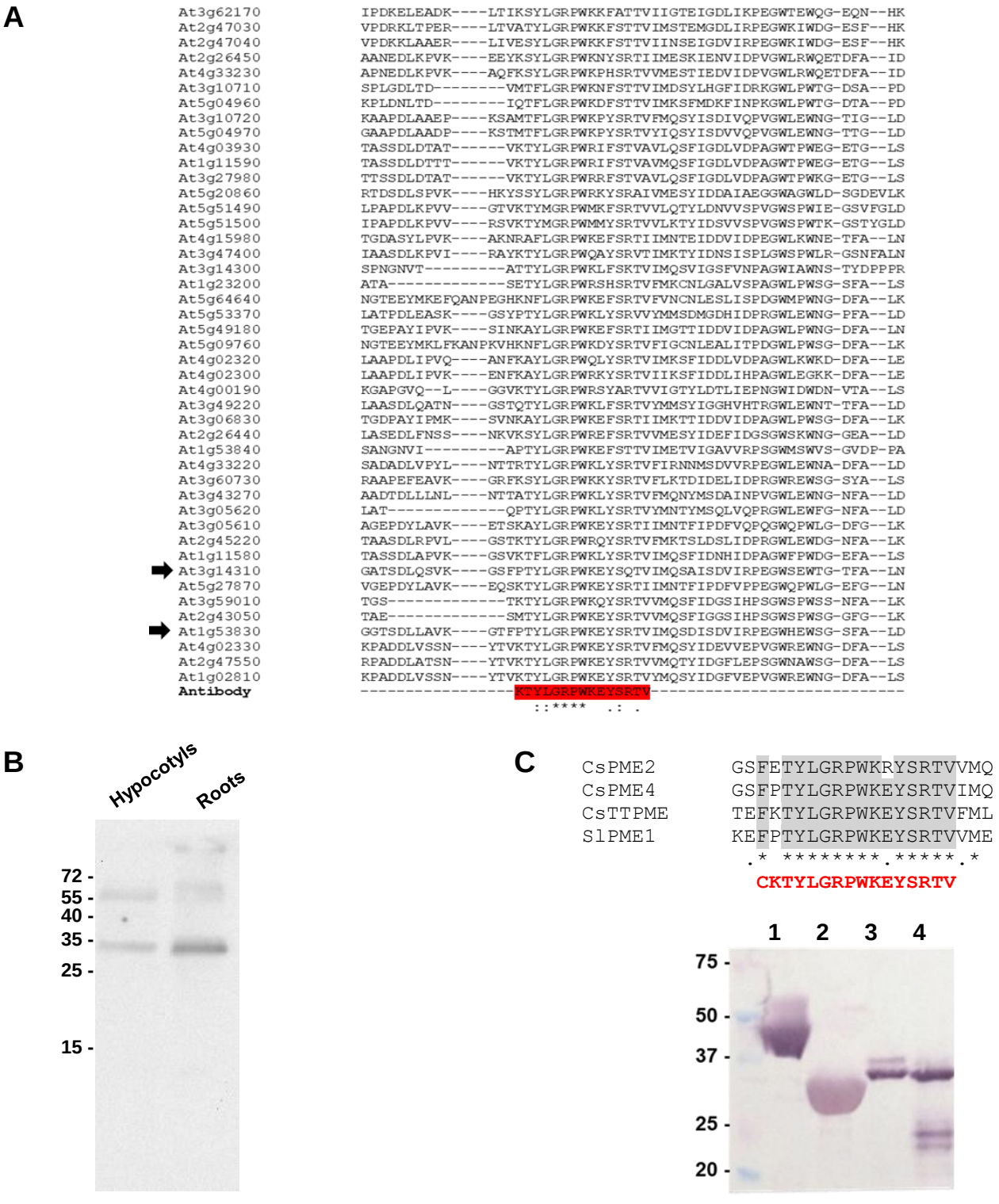

Supplemental Figure 6: (A) Sequence alignment of 45 Arabidopsis PME isoforms showing the conservation of the epitope used for production of the generic anti-PME antibody. **(B)** Western blot analysis of cell- wall-enriched protein extracts from 7 day-old roots and 4 day-old dark grown hypocotyls using the designed anti-PME peptide antibody. Both processed (~35kDa) and non-processed (~55kDa) forms of PME can be detected. **(C)** Sequence alignment of previously characterized PMEs from Citrus and Solanum showing the conservation of the epitope. Western blot analysis of purified PMEs, 1: CsTT-PME (Citrus sinensis thermally-tolerant isozyme; (Savary et al., 2013)), 2: CsPME2 (C. sinensis fruit-specific salt-independent isozyme, (Savary et al., 2010), 3: CsPME4 (C. sinensis salt-dependent isozyme, (Savary et al., 2010)), and SlPME1 (Solanum lycopersicum isozyme (Savary, 2001)).

PRO-region sequence (~30 kDa)

```
  1 MAPIKEFISK FSDFKNNKKL ILSSAAIALL LLASIVGIAA TTTNQNKNQK
 51 ITTLSSTSHA ILKSVCSSTL YPELCFSAVA ATGGKELTSQ KEVIEASLNL
101 TTKAVKHNYF AVKKLIAKRK GLTPREVTAL HDCLETIDET LDELHVAVED
151 LHQYPKQKSL RKHADDLKTL ISSAITNQGT CLDGFSYDDA DRKVRKALLK
201 GQVHVEHMCS NALAMIKNMT ETDIANFELR DKSSTFTNNN NRKLKEVTGD
251 LDSDGWPKWL SVGDRRLL
```

Catalytic region sequence (~35 kDa)

```
                       QG STIKADATVA DDGSGDFTTV AAAVAAAPEK
301 SNKRFVIHIK AGVYRENVEV TKKKTNIMFL GDGRGKTIIT GSRNVVDGST
351 TFHSATVAAV GERFLARDIT FQNTAGPSKH QAVALRVGSD FSAFYQCDMF
401 AYQDTLYVHS NRQFFVKCHI TGTVDFIFGN AAAVLQDCDI NARRPNSGQK
451 NMVTAQGRSD PNQNTGIVIQ NCRIGGTSDL LAVKGTFPTY LGRPWKEYSR
501 TVIMQSDISD VIRPEGWHEW SGSFALDTLT YREYLNRGGG AGTANRVKWK
551 GYKVITSDTE AQPFTAGQFI GGGGWLASTG FPFSLSL
```

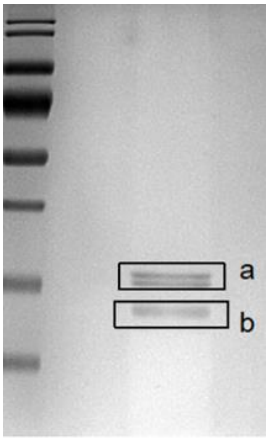

Catalytic region tryptic peptides – 12 observed (2 truncated) (“Band a”)

Position	Peptide sequences
75-300	ADATVADDGSGDFTTVAAAVAAAPEK*
316-322	ENVEVTK*
325-334	TNIMFLGDGR
344-363	NVVDGSTTFHSATVAAVGER
368-379	DITFQNTAGPSK
387-412	VGSDFSAFYQCDMFAYQDTL YVHSNR
451-458	NMVTAQGR
459-473	SDPNQNTGIVIQNCR*
474-484	IGGTSDLLAVK*
485-496	GTFPTYLGRPWK*
501-532	TVIMQSDISDVIRPEGWH (+EWSGSFALDTLTYR) – fragment observed
554-587	VITSDTEAQPFTAGQFIGGG (+GWLASTGFPFSLSL) – fragment observed

PRO-region tryptic peptides – 7 observed (“Band b”)

Position	Peptide sequences
51-63	ITTLSSTSHAILK
64-85	SVCSSTLYPELCFSAVAATGGK
107-113	HNYFAVK
169-192	TLISSAITNQGTCLDGFSYDDADR
201-217	GQVHVEHMCSNALAMIK
218-230	NMTETDIANFELR
233-242	SSTFTNNNNR

*Peptides observed in cell wall extract and indicated by sequence alignment in Supp Fig 1

Supplemental Figure 7: Identification of peptides mapping the PRO and mature (catalytic) regions of AtPME2 following cation exchange purification. Band **a** corresponds to the two isoforms at ~35 kDa while band **b** corresponds to the band below ~35kDa (see gel).

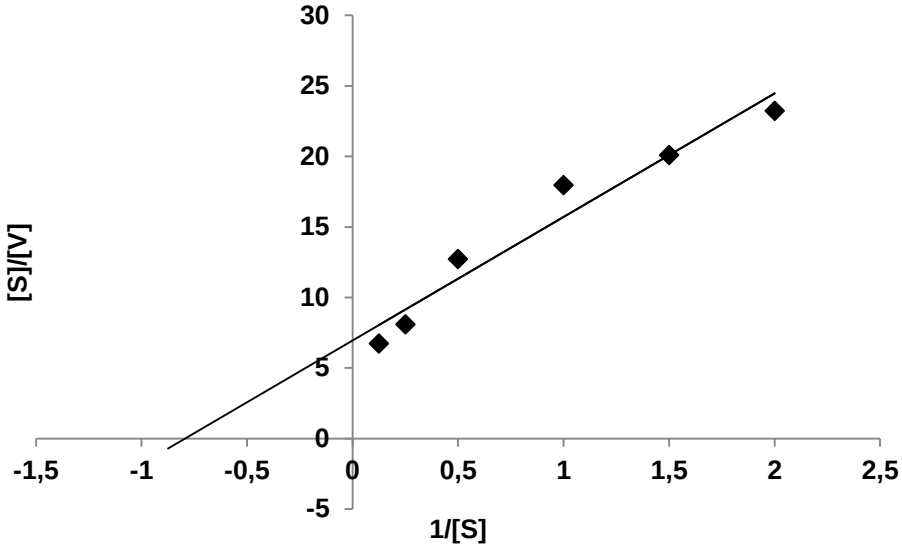

Supplemental Figure 8: Determination of Km and Vmax for AtPME2. Activity was assessed using various concentrations of pectins DM 55-70% at 37°C and pH 7.5. [S] is expressed in $mg.mL^{-1}$ and [V] in $nmol.MeOH.min^{-1}.\mu g.prot^{-1}$.

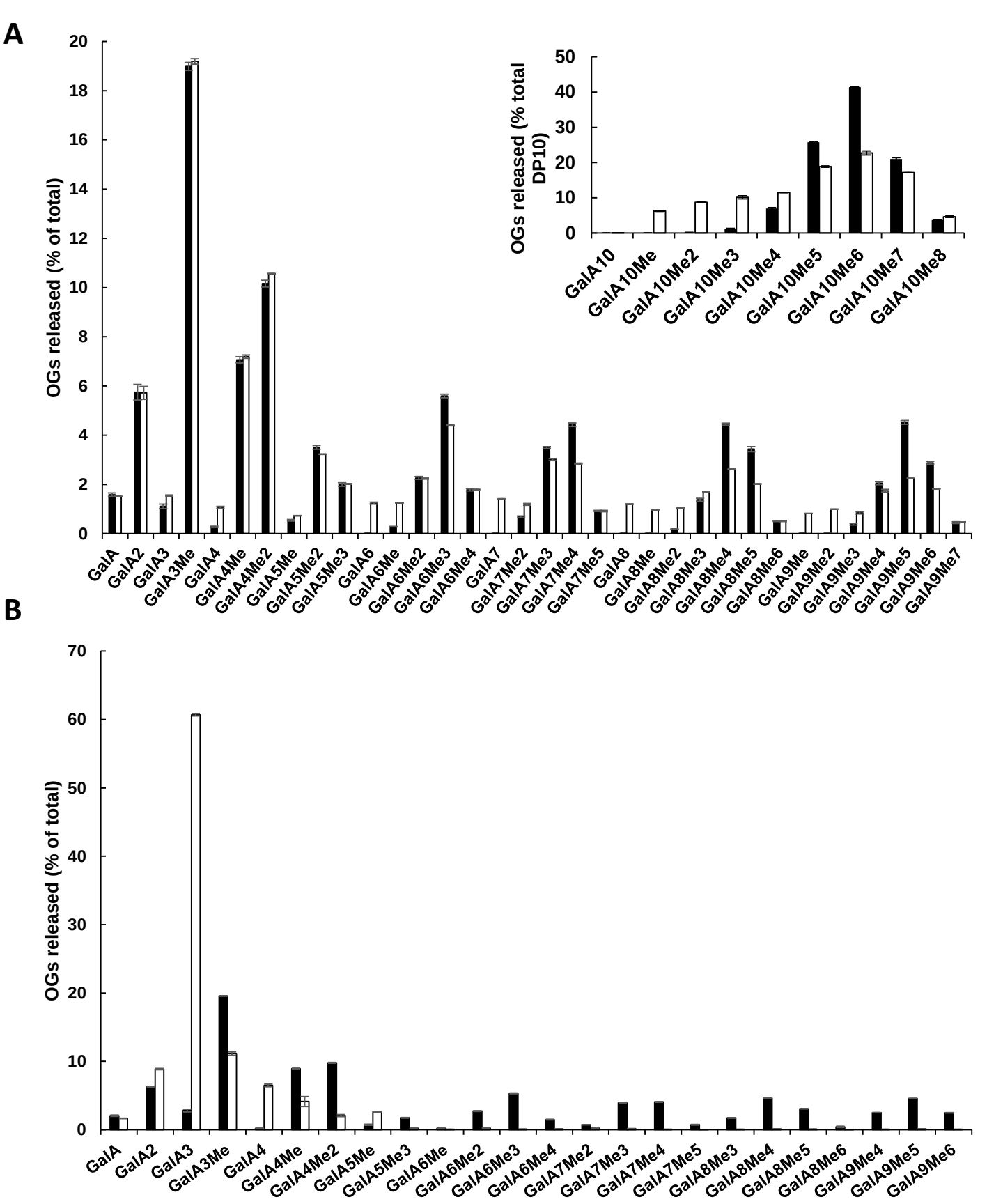

Supplemental Figure 9: Determination of the processivity of CsPME at **(A)** pH 5 and (**B**) pH 8 using LC-MS/MS. Non-digested samples (black bars); CsPME digestion (white bars). Data represent the mean ± SE of three replicates.

		Col-0		WS	
		% coverage	Nb peptides	% coverage	Nb peptides
AT1G30600.1	Subtilase family protein			8,65	4
AT1G32940.1	Subtilase family protein	20,8	14		
AT1G53830.1	**Pectin methylesterase 2**	18,91	5	16,87	4
AT2G04160.1	Subtilisin-like serine endopeptidase	15,16	9	18,39	11
AT2G05920.1	Subtilase family protein	62,2	29	62,2	30
AT2G45220.1	Plant invertase/pectin methylesterase inhibitor	30,53	13	31,12	13
AT3G14067.1	Subtilase family protein	38,87	17	38,35	17
AT3G14310.1	Pectin methylesterase 3	23,99	8	19,93	7
AT3G16850.1	Pectin lyase-like superfamily protein	18,46	5	17,58	5
AT3G43270.1	Plant invertase/pectin methylesterase inhibitor			11,2	3
AT3G57790.1	Pectin lyase-like superfamily protein			14,69	7
AT4G19410.1	Pectinacetylesterase family protein	63,94	14	47,39	14
AT4G20430.2	Subtilase family protein	4,21	2	4,21	2
AT4G21650.1	Subtilase family protein			11,1	6
AT4G23500.1	Pectin lyase-like superfamily protein	4,65	2	12,53	4
AT4G25260.1	Plant invertase/pectin methylesterase inhibitor			11,94	2
AT4G33220.1	pectin methylesterase 44			13,9	3
AT4G34980.1	Subtilase family protein	18,85	11	23,04	13
AT5G09760.1	Plant invertase/pectin methylesterase inhibitor	13,43	5	11,8	5
AT5G44530.1	Subtilase family protein	13,81	7	9,05	4
AT5G45280.2	Pectinacetylesterase family protein	47,83	10	43,22	10
AT5G59090.2	Subtilase 4.12	30,23	16	35,15	21
AT5G62350.1	Plant invertase/pectin methylesterase inhibitor			36,63	4
AT5G67360.1	Subtilase family protein	32,76	17	42,8	21

Supplemental Table I: Identification of homogalacturonan remodeling enzymes and regulators in cell wall-enriched protein extracts of Col-0/WS roots.

Genotyping	
pme2-1 F	5’-GACGGAAGCGGTGACTTTAC-3’
pme2-1 R	5’-AGTGTCCAACGCAAAACTCC-3’
pme2-2 F	5’-CTCAACACTATACCCGGA-3’
pme2-2 R	5’-ACTTTCCTATCGGCGTCG-3’
GK F	5’-ATATTGACCATCATACTCATTGC-3’
FLAG F	5’-CTACAAATTGCCTTTTCTTATCGAC-3’
RT-qPCR	
AtPME2 F	5’-TACGACGACGCCGATAGGAAAG-3’
AtPME2 R	5’-ATGTGCTCCACGTGTACCTGAC-3’
APT1 F	5’-GAGACATTTTGCGTGGGATT-3’
APT1 R	5’-CGGGGATTTTAAGTGGAACA-3’
CLA F	5’-GTTTGGGAGAAGAGCGGTTA-3’
CLA R	5'-CTGATGTCACTGAACCTGAACTG-3'
TIP41 F	5’-GCTCATCGGTACGCTCTTTT-3’
TIP41 R	5’-TCCATCAGTCAGAGGCTTCC-3’
Promoter cloning	
primer F	5’-**AAGCT**TGTACAATGATGGTTCTATTGT-3’
primer R	5’-**TCTAGA**GGTGGAATAGGGTTTATATTG-3’
CDS cloning for confocal imaging	
primer F	5’-**CACC**ATGGCACCAATCAAAG-3’
primer R	5’-AAGACTTAACGAGAAAGGAA-3’
CDS cloning for Pichia expression	
primer F	5'-**CTGCAG**GAGCCACAACAACAAAC-3'
primer R	5'-**GCGGCCG**CAAGACTTAACGAGAAAGGA-3'

Supplemental Table II: Primers used in the study.

Parameter	Value used	Default value
Image channel	Green	No
Spatial resolution	20.55µm	No
Time interval	120 min	No
Smoothing method	Box filter	Yes
Radius	2	Yes
Threshold	Automatic	Yes
Threshold method	Max entropy	Yes
Smoothing factor for contours	20	Yes
First point of skeleton	Bottom	Yes
Curvature smoothing	10	Yes
Number of points for resampling	500	Yes
Channel for computing displacement	Green	No
Step between two measurements of displacements	1	No
Size of the correlating window #1	5	Yes
Spatial smoothing	0.1	Yes
Value smoothing	0.05	No
Resampling distance	0.05	No
Size of the correlating window #2	20	Yes

Supplemental Table III: Parameters used for spatial growth pattern determination using KymoRod (Bastien et al. Plant J 2016).